PERMEABILITY OF ARTIFICIAL MEMBRANES TO A PLURIDISPERSE SOLUTION OF ^{125}I-POLYVINYLPYRROLIDONE

ROBERT DU BOIS *and* ERIC STOUPEL

From the Laboratory for Experimental Medicine, Brussels University and Queen Elizabeth Foundation, Brussels, Belgium

ABSTRACT The validity of the transport equation for uncharged macromolecules across a porous membrane developed by Verniory et al. (1973, *J. Gen. Physiol.* **62**:489) has been tested on several types of artificial membranes (Amicon PM-30, XM-50, and XM-100 Diaflo ultrafilters) using a pluridisperse solution of polyvinylpyrrolidone as filtrand. The influence of the filtration pressure on the shape of the sieving curve predicted by the theory has been verified. A mean pore radius and the width of the pore radii distribution function have been calculated from the sieving data. It has been demonstrated that the method used previously to determine the effective filtration pressure in the glomerulus from sieving data is valid. The transport equation previously proposed by Renkin (1954, *J. Gen. Physiol.* **38**:225) gives results that are less consistent than those obtained with the new transport equation.

INTRODUCTION

The pore theory of membrane transport has received considerable attention since the pioneering work of Pappenheimer et al. (2). According to this theory, both convection and diffusion contribute to solute transport across the porous membrane, the two processes being impeded by steric hindrance at the entrance of the pores and by frictional forces within the pores; the same steric hindrance and frictional resistance terms were used in the convection and diffusion terms of the solute transport equation.

We have shown previously (1) that both the steric hindrance and the frictional resistance terms should in fact be different for convection and diffusion. The same conclusion was reached independently by Bean (3) in his comprehensive review of the physics of porous membranes. The transport equation in this modified form has been used independently by Chang et al. (4) and by Lambert et al. (5) for their studies of hemodynamical parameters and permeability properties of renal glomeruli.

The accuracy of the diffusion term of the transport equation has been verified by the careful experimental work of Beck and Schultz (6), using track-etched mica membranes having pores of well-defined radius and length. The accuracy of the new convection term has not yet been tested since Renkin (7), in the only ultrafiltration experiments comparable to the present study, used the same frictional resistance term for both convection and diffusion.

In order to test more completely the transport equation, we have studied the transport of the solute under the combined influence of diffusion and convection. Mica membranes, though possessing a nearly ideal pore structure, are very fragile and therefore not very suitable for ultrafiltration studies. Amicon Diaflo membranes (Amicon Corp., Lexington, Mass.) were selected for the experiments because pores of nearly circular cross-section have been demonstrated by electron microscopy. Also, several types of membranes with different radii are available.

The solute is a pluridisperse preparation of radioactively labeled polyvinylpyrrolidone (PVP). Tracer quantities of PVP were used to minimize pore plugging and interaction between macromolecules. Fractions of different molecular sizes in filtrate and filtrand can be separated by gel column chromatography. The use of a pluridisperse solution is interesting because the whole sieving curve (plot of the ratios of filtrate to filtrand solute concentrations against molecular radius) can be calculated from a single sample of filtrate. The information obtained in this way is more complete than that which is obtained by using several solutes with different radii, and probably more reliable. Indeed, molecules of PVP of different sizes can be expected to have more similar properties than, for example, proteins, which can take on various shapes. Further, PVP molecules are uncharged while proteins are charged.

In the theoretical part of this work, two extensions of the theory will be proposed: (*a*) the transport equation established previously for an isoporous membrane (1) is modified for the case of a heteroporous membrane; and (*b*) the radial variation of the frictional resistance factor for convection is taken into account; this variation was experimentally demonstrated by Goldsmith and Mason (8) and their experimental data were used to estimate the magnitude of this effect.

Our experimental work was mainly devoted to the determination of sieving curves of PVP at different filtration pressures and on several types of Amicon membranes. The analysis of the experimental data leads to the following conclusions: (*i*) the influence of the filtration pressure on the shape of the sieving curve predicted by the theory is verified; (*ii*) the parameters characterizing the porosity of the membranes (mean pore radius and width of the pore radii distribution function) can be derived from the sieving data; (*iii*) the method used in our laboratory to determine the effective glomerular filtration pressure in the dog from the sieving of PVP through the glomerular membrane is validated.

LIST OF SYMBOLS

a	Radius of solute molecules (Å)
c_1, c_2	Solute concentrations in filtrand and filtrate ($mol \cdot ml^{-1}$)
D	Free diffusion coefficient of solute ($cm^2 \cdot s^{-1}$)
$j_s(J_s)$, $j_v(J_v)$	Solute, solvent flows per second and square centimeter of membrane for isoporous (heteroporous) membrane (mol or $ml \cdot s^{-1} \cdot cm^{-2}$)
K_1, K_2	Wall correction factors (dimensionless)
K_{av}	Partition coefficient of a fraction on chromatography column (dimensionless)
L	Length of pores (cm)
L_p	Hydraulic conductance of the membrane ($ml \cdot min^{-1} \cdot cm^{-1}$ $H_2O \cdot cm^{-2}$)

N	Number of pores per square centimeter of membrane (cm^{-2})
r	Pore radius (Å)
r_h, s	Median and standard deviation of lognormal pore radius distribution (Å)
r_m	Mean pore radius, Eq. 10 (Å)
S_D, S_F	Steric hindrance factors for diffusion, filtration, Eqs. 4 and 5 (dimensionless)
V_e, V_o, V_t	Elution volumes of fraction, of blue dextran, of KCl (ml)

Greek Letters

ΔP	Pressure gradient across membrane or effective filtration pressure ($dyn \cdot cm^{-2}$ or cm H_2O
η	Dynamic viscosity ($dyn \cdot s \cdot cm^{-2}$)
θ	Total pore area per square centimeter of membrane (dimensionless)
ρ	Distance from pore axis (Å)
ΣE	Sum of weighted quadratic errors (dimensionless)
φ, φ_h	Sieving coefficients, Eqs. 2 and 13 (dimensionless)

THEORY

Sieving Coefficient for an Isoporous Membrane

In this section, we shall recall only the theoretical equations necessary for the interpretation of our experimental data. Their derivation is given in ref. 1.

The artificial membrane is assimilated to an assembly of straight circular pores of uniform radius r and length L (L is much greater than r); the number of pores per square centimeter of membrane is N; the solute molecules are simulated by rigid spheres of radius a (a and r are much greater than the radius of the solvent molecules). The solute concentration in the filtrand is c_1, that in the filtrate c_2. A filtration pressure ΔP is applied across the membrane. The hydraulic conductance of the membrane L_p is given by Poiseuille's law:

$$L_p = N\pi r^4/8\eta L = \theta r^2/8\eta L, \tag{1}$$

where η is the dynamic viscosity of the solvent and θ the pore area per square centimeter of membrane, numerically equal to $N\pi r^2$.

It is assumed that the following conditions are satisfied in the experiments:

(*i*) The Reynolds number of the solvent flow is very low; then the velocity profile in the pores, far from any solute molecule, is parabolic, and it is established at the very beginning of the pores.

(*ii*) The filtration rate is constant.

(*iii*) The solute concentrations are sufficiently low, so that there is no interaction among solute molecules in the pores; then, the solvent flow is hardly modified by the presence of the solute molecules.

The sieving coefficient φ of molecules of radius a, is defined as the ratio of solute clearance (solute mass flow divided by c_1) to solvent volume flow. It is equal to c_2/c_1. As shown in ref. 1

$$\varphi = S_F(K_2/K_1)/1 - e^{-K}[1 - S_F(K_2/K_1)], \tag{2}$$

where $K = S_F K_2 j_v L / S_D D$. D is the diffusion coefficient of the solute. j_v is the solvent volume flow per second and per square centimeter of the membrane; as the solute concentrations are very low, the osmotic effects of the solute are negligible and

$$j_v = L_p \Delta P. \tag{3}$$

S_D and S_F, the steric hindrance factors for diffusion and convection are given by Eqs. 4 and 5:

$$S_D = (1 - a/r)^2, \tag{4}$$

$$S_F = S_D(2 - S_D). \tag{5}$$

K_1 and K_2, the "wall correction factors," describe the enhancement of the drag forces on the solute molecules due to the pore walls. If one neglects direct interactions between solute and pore walls, such as collisions due to Brownian motion, and in the absence of electric effects, K_1 and K_2 are defined as the ratios of the drag forces felt by, respectively, (*a*) a sphere moving in a stationary liquid and (*b*) a stationary sphere in a moving liquid to the drag in an infinite medium. K_1 and K_2 depend only on the dimensionless factors a/r and ρ/r (ρ is the distance of the solute molecule's center to the pore axis).

Eq. 2 was established with the assumption that K_1 and K_2 did not depend on ρ/r and had everywhere their axial values, K_1' and K_2'. Anderson and Quinn (9) have shown that one can take into account the radial variation of K_1^{-1} and K_2/K_1 by using suitably averaged values of these quantities over the available pore area, $\overline{K_1^{-1}}$ and $\overline{K_2/K_1}$ ($\overline{K^{-1}}$ and $\overline{G}$ in their notation) defined as follows:

$$\overline{K_1^{-1}} = (1/S_D)(1/\pi r^2) \int_0^{r-a} (2\pi\rho d\rho / K_1), \tag{6}$$

$$\overline{K_2/K_1} = (1/S_F)(1/\pi r^2) \int_0^{r-a} 2\pi\rho (K_2/K_1)[1 - (\rho^2/r^2)] d\rho. \tag{7}$$

$S_D\overline{K_1^{-1}}$ and $S_F\overline{K_2/K_1}$ are equal to the parameters ξ and χ defined by Anderson and Quinn (9); they correspond to the parameters ω/ω_o and $1 - \sigma$ used in the thermodynamic description of solute transport through neutral membranes.

Radial variation of K_1 and K_2

Many theoretical papers have been devoted to the calculation of the drag force on a sphere in a cylinder, in the absence or presence of flow. Most papers have only considered the special case of a sphere moving along the cylinder's axis. Haberman and Sayre (10) have calculated K_1 and K_2 for axial spheres of radius $a \leq 0.8\ r$; Wang and Skalak (11) have extended these results up to $0.9\ r$. In addition to approximate analytical formulas (valid up to $a = 0.6\ r$ and quoted in ref. 1), Haberman and Sayre give the following exact values for $a/r = 0.1$ up to 0.8: K_1 = 1.263, 1.680, 2.371, 3.596, 5.970, 11.135, 24.955, 73.555; K_2 = 1.255, 1.635, 2.231, 3.218, 5.004, 8.651, 17.671,

47.301. More recently, Paine and Scherr calculated K_1 and K_2 over the range $0 < a/r \leq 0.9$ in 0.02 unit intervals (12).

The drag force on a sphere moving off-axis has been calculated by Famularo (ref. 13, quoted in ref. 14, p. 309), by Brenner and Happel (15), by Brenner and Bungay (16), and by Greenstein and Happel (17), but only for small values of a/r (lower than 0.1, for instance). K_1 was shown to be relatively constant for ρ/r up to 0.6.

Bungay and Brenner have studied two other particular situations: (*a*) a small sphere in close proximity to the cylinder's wall, i.e. $a \leq r - \rho \ll r$ (18); (*b*) a closely-fitting sphere, i.e. $a \leq \rho \leq r$, a of the order of r (19). Some of these theoretical results from fluid dynamics have been used to calculate $\overline{K_1^{-1}}$ and $\overline{K_2/K_1}$.

Bean (3) used the results of Famularo to calculate $\overline{K_1^{-1}}$ and found that the frictional resistance to diffusion was significantly larger than that predicted by the axial value of $K_1'^{-1}$. Bean also cited unpublished experiments with R. W. De Blois and D. C. Golibersuch that lead to the conclusion that K_2/K_1 (G in Bean's notation) is very uniform off the axis.

Starting from Greenstein and Happel results, Levitt (20) draws a different conclusion: he found $\overline{K_1^{-1}}$ very close to $K_1'^{-1}$; while $\overline{K_2/K_1}$ was found only slightly different from Bean's value.

Anderson and Quinn (9) derived a composite formula for the drag off-axis, combining the results of Famularo (sphere in a cylindrical tube) and those of Goldman et al. (21) for a sphere moving parallel to a flat wall. They found, like Bean, a significant effect on $\overline{K_1^{-1}}$ and only a small difference between $\overline{K_2/K_1}$ and the axial value.

However, as already pointed out, these calculations are based on theoretical results which are valid only for small values of a/r; therefore, one expects them to be strictly valid only in this range.

In our experiments, $a/r > 0.3$. If we are to take into acount the radial variation of K_1 and K_2, we need to know the values of these factors for $0.3 \leq a/r < 1.0$ and $0 \leq \rho/r \leq 1 - a/r$ (the center of the sphere cannot come closer to the wall than a). For this range of values of a/r and ρ/r, there are at present no theoretical results. We have thus turned to experimental data. Beck and Schultz (6) have measured the restricted diffusion of various small nonelectrolytes in pores consisting of etched particle tracks in mica. Their results (discussed by Bean [3], p. 30) indicate that the axial approximation for $\overline{K_1^{-1}}$ is quite reasonable. We shall thus use the axial approximation for K_1^{-1}.

Goldsmith and Mason (8) studied the motion of macroscopic polystyrene spheres suspended in a liquid undergoing laminar viscous flow in a cylinder. The relative velocity u'/u of the neutrally buoyant spheres (u' is the measured velocity of the sphere and u the streamline velocity of the fluid at the same distance from the axis as the center of the sphere) is equal to K_2/K_1. The velocities of various spheres of radius a between 0.1 and 0.53 r moving at different distances from the axis ($0 \leq \rho/r \leq 0.81$) were determined.

The analysis of the experimental data shows that the radial variation of K_2/K_1 is the same for spheres of different a/r. This property probably accounts for the reason-

able agreement found by Bungay and Brenner (18) between their theoretical predictions (obtained by the method of reflections expansion, and valid for small a/r) and the experimental data of Goldsmith and Mason (a/r between 0.1 and 0.5).

We have fitted by the least squares method an empirical curve to all available experimental results of Eq. 8 for $\rho/r \leq 0.6$. The following formula was found:

$$K_2/K_1 = 1 - (1 - K_2'/K_1')(1 + 12.47\,\rho^4/r^4). \quad (8)$$

Introducing Eq. 8 into Eq. 7, we find:

$$\overline{K_2/K_1} = 1/S_F\{2S_D(K_2'/K_1') - S_D^2(K_2'/K_1') + 8.31\,S_D^3[(K_2'/K_1') - 1] + 6.24\,S_D^4[1 - (K_2'/K_1')]\}. \quad (9)$$

The axial value K_2'/K_1' is compared with the averaged value $\overline{K_2/K_1}$ in Fig. 1 A. The full line represents $\overline{S_F K_2/K_1}$ while the dashed line shows $S_F K_2'/K_1'$ in function of a/r. For comparison, the restriction term S_F/K_1 used by Renkin (7) is also shown. The restriction predicted by Renkin's term is much greater than that predicted by both other formulas.

Fig. 1 B illustrates the theoretical effect of ΔP (equal to j_v/L_p) on the shape of the sieving curve (plot of φ in function of a/r). The steepness of the central part of the curve is greater for lower pressures and it is thus to be expected that the membrane will be more selective, i.e. will better be able to separate solutes of similar sizes at

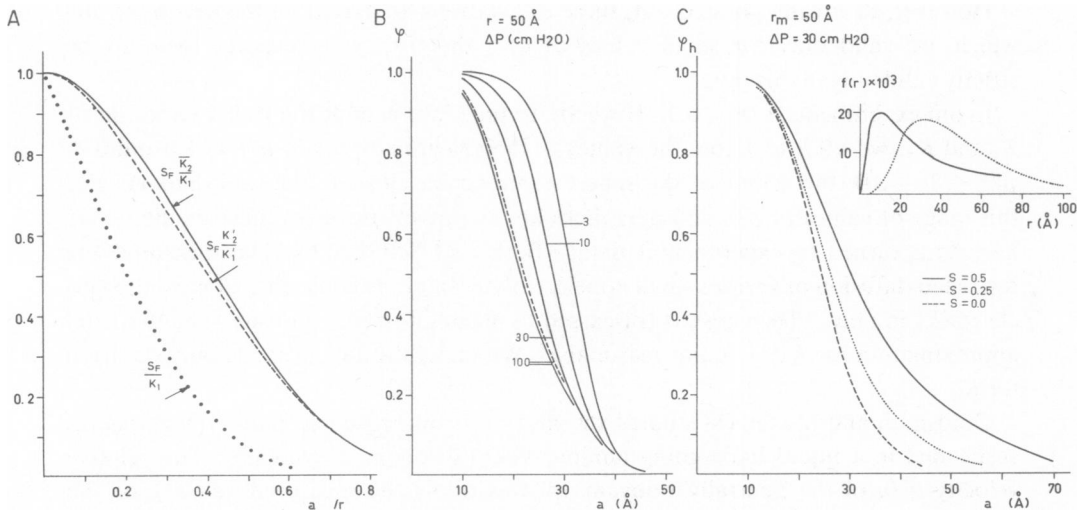

FIGURE 1 (*A*) Values of $S_F\,\overline{K_2/K_1}$ in function of a/r; solid line, taking into account the radial variation of K_2/K_1, Eq. 9; dashed line, axial approximation. Renkin's term S_F/K_1 is also shown. (*B*) Solid lines: theoretical sieving curves for an isoporous membrane (r = 50 Å) at different filtration pressures; $\overline{K_2/K_1}$ given by Eq. 9. Dashed line: curve for ΔP = 100 cm H_2O, axial approximation. (*C*) Theoretical sieving curves for heteroporous membranes with same r_m; s = 0 corresponds to an isoporous membrane.

low pressures. The full lines correspond to Eq. 2 with $\overline{K_2/K_1}$ given by Eq. 9 while the dashed line shows the curve corresponding to ΔP = 100 cm H_2O in the axial approximation. At lower pressures, the radial correction becomes negligible as the relative part of convection becomes smaller.

Sieving Coefficient for an Heteroporous Membrane

To interpret our experimental data, it was found necessary to calculate the sieving coefficient for an heteroporous membrane. The extension of the theory to this case is straightforward.

Let $f(r)$ be the distribution function of the radii of the pores, with $\int_0^\infty f(r)\mathrm{d}r = 1$. We shall define the mean pore radius r_m as the radius of an isoporous membrane having the same number of pores per square centimeter N and same hydraulic conductance as the heteroporous membrane considered. Since, according to Poiseuille's law, the flow in a cylinder is proportional to the fourth power of its radius,

$$r_m = \left\{\int_0^\infty r^4 f(r)\mathrm{d}r\right\}^{1/4}. \tag{10}$$

The sieving coefficient φ_h is equal to $J_s/c_1 J_v$. The mean solvent and solute flows per second and square centimeter, J_v and J_s, are given by Eqs. 11 and 12:

$$J_v = \int_0^\infty f(r)\, j_v \mathrm{d}r = N \int_0^\infty \frac{\Delta P \pi r^4}{8\eta L} f(r)\mathrm{d}r, \tag{11}$$

$$J_s = \int_0^\infty f(r)\, j_s \mathrm{d}r = \mathrm{N} \int_0^\infty \frac{\overline{K}_2}{K_1} \frac{\Delta P \pi r^4 S_F(c_2 - c_1 e^K)}{8L\eta(1 - e^K)} f(r)\mathrm{d}r. \tag{12}$$

j_s is the solute flow per second and square centimeter for an isoporous membrane (Eq. 20 of ref. 1 where the term containing $\overline{V_s}$ is neglected); j_v is given by Eq. 3 of the present work.

As the Amicon membranes that we used are anisotropic (the thin filtering "skin" being laminated to a porous structure of the same polymer), and as they are supported by a porous disc, the liquid at the exit of the pores is not well mixed, and pores of unequal radii will produce filtrate with unequal solute concentrations. c_2 in Eq. 12 is replaced by c_1 with φ given by Eq. 2, and φ_h becomes

$$\varphi_h = \frac{\int_0^\infty f(r) S_F(\overline{K_2/K_1}) r^4 [e^K/(e^K - 1)]\mathrm{d}r}{\int_0^\infty f(r) r^4 [1 + S_F(\overline{K_2/K_1})/e^K - 1]\mathrm{d}r}. \tag{13}$$

Theoretical sieving curves, calculated according to Eq. 13, for lognormal pore distribution functions of different standard deviations s but same r_m (equal to 50 Å) are shown in Fig. 1 C, together with the distribution curves. For these calculations, and other computations in this article involving $f(r)$, the lognormal distribution is ap-

proximated by five classes of pores with radii r_h exp (ns), with $n = -2$ up to $+2$, and relative pore numbers 0.0668, 0.2417, 0.383, 0.2417, 0.0668. r_h represents the median pore radius of the lognormal distribution. These developments closely parallel those of Lambert et al. (22).

MATERIAL AND METHODS

Membrane

Diaflo PM-30, XM-50 and XM-100 A ultrafilters (Amicon Corp., Lexington, Mass.) were used in the experiments. The membranes are anisotropic and nonionic; they consist, according to the manufacturer, of a 0.1–1.5 μm thick skin of controlled pore texture upon a much thicker, 50–250 μm spongy layer of the same polymer. The surface structure of the XM-50 and XM-100 was studied by Preusser (23) with an electron microscope. Almost circular pores, with a narrow width pore size distribution, and maxima for radii of 46 Å (XM-50) and 70 Å (XM-100) were observed. The length and shape of the pores inside the membrane are not revealed by this technique.

Solute

The permeating substance is a pluridisperse preparation of radioactively labeled polyvinylpyrrolidone ([^{125}I]PVP at 0.5 mg%) (Radio Chemical Centre, Amersham, England) dissolved in distilled water or 0.9% saline. The range of molecular weights is 10,000–85,000, with a mean mol wt of 33,000. It is found by chromatography (see section on Determination of the Sieving Curve) that this corresponds to hydrodynamically equivalent radii between 10 Å and 90 Å. Unlabeled PVP (2.5 mg%) and NaI (0.3 mg%) are added to the solution to minimize losses of the tracer substance by adsorption in the experimental apparatus and during chromatography. The solute concentration is low enough to satisfy assumption *iii* (Theory section, above).

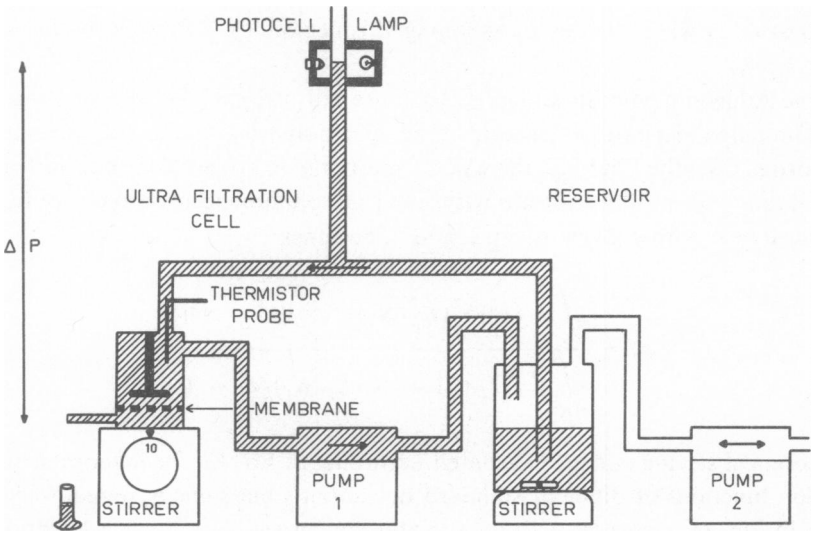

FIGURE 2 Experimental apparatus.

Experimental Apparatus

Fig. 2 shows a diagram of the experimental apparatus. The 50 ml ultrafiltration cell (Amicon model 52) is placed on top of a magnetic stirring table operating at full speed (Amicon model MT2) in order to get an homogeneous concentration in the filtrand compartment and to prevent the formation of unstirred layers. To minimize the variation of the solute concentration in the filtrand during the experiment, the solution of a reservoir of about 600 ml is circulated through the cell.

The membrane is supported by a porous disc so that the entire membrane area can be used. The void volume of the cell (under the membrane) plus the porous support plus the output tubing is less than 2 ml.

The filtration pressure is measured by means of a water gauge. It is kept within ± 0.2 cm H_2O of the desired pressure by a lamp and phototransistor which control the height of the liquid in the column by activating the peristaltic pump P_2 which injects or extracts air from the reservoir to compensate for loss of water through the ultrafiltration process and for temperature changes.

As such, the apparatus allows pressures between 5 and 150 cm H_2O to be maintained indefinitely. For higher pressures, the apparatus was slightly modified and the water gauge replaced by a mercury gauge.

The temperature in the cell is monitored by a thermistor probe (Tele-Thermometer, Yellow Springs Instruments Co., Yellow Springs, Ohio). Temperature changes during the collection of samples were smaller than 1°C, except for the samples collected at the lowest pressures (< 10 cm H_2O), where, due to a greater collection time, variations were more important, but always smaller than 3°C.

Determination of the Sieving Curve

The conductance of the membrane is measured at different pressures, with distilled water. All XM-50 membranes had to be pressurized to about 1 atm to initiate water flow.

Then, the PVP solution is introduced in the reservoir and circulated through the cell for several hours. After this, samples of filtrate are taken at various pressures. Whenever the pressure is changed, a volume of 5 ml of filtrate, more than twice the void volume of the cell, is discarded before collecting a sample.

The samples of filtrate and filtrand are chromatographed successively on the same K26/40 column (Pharmacia Fine Chemicals, Uppsala, Sweden) of Sephadex G 200 (Pharmacia, quality: fine) with saline as buffer. The eluted fractions are collected with an automatic fractionator (Ultrorac, model 7000, LKB, Bromma 1, Sweden). The activities of the fractions are determined in an automatic Gamma analyser (Philips, Eindhoven, Holland).

The mean hydrodynamically equivalent molecular radius a of each fraction of filtrate and filtrand is calculated by Eq. 14:

$$\log a = A(1 - K_{av}) + B, \tag{14}$$

where $K_{av} = (V_e - V_o)/(V_t - V_o)$, V_e is the elution volume of the fraction, V_o and V_t, respectively, the void volume (taken equal to the elution volume of blue dextran) and the total volume (elution volume of KCl) of the column. The coefficients A and B are determined for each column by chromatographing 11 proteins of well-known molecular sizes[1] (Sigma Chemical Co.,

[1]Bovine pancreas ribonuclease Type IA; horse heart cytochrome C Type III; equine skeletal muscle myoglobin Type I; bovine pancreas trypsin Type III; bovine pancreas chymotrypsin Type II; ovalbumin; human hemoglobin Type IV; horseradish peroxidase Type I; calf intestinal mucosa alkaline phosphatase; human serumalbumin; human transferrin and human γ-globulin.

St. Louis, Mo.). For 12 columns, the following values were found:

$$A = 0.900, \text{ and } B = 0.983.$$

The range of K_{av} values where Eq. 14 is valid is approximately 0.2 to 0.8; this corresponds to radii between 15 and 50 Å.

The sieving coefficient of molecules of a given size is the ratio of the number of counts in the corresponding fractions of filtrate and filtrand. The sieving coefficients for integer values of the molecular radius are calculated by logarithmic interpolation. The sieving curve can then be drawn. These calculations are repeated for all filtrate samples.

Computer Methods

It has been shown in the theoretical part that for an isoporous membrane, the shape of the sieving curve depends on the radius of the pores and on the filtration pressure. For an heteroporous membrane, one or more parameters may influence the shape. We chose to consider a lognormal distribution, where only one additional parameter, the standard deviation of the distribution, needs to be considered.

As the filtration pressure is known for each experiment, the other parameters can be determined by fitting, with the help of a computer (CDC 6500 of the Brussels' Universities Computation Center) the theoretical curve to the experimental results.

The computer program finds the values of the parameters minimizing the sum of weighted quadratic errors

$$\sum E = \sum_i (\varphi_i^* - \varphi_i)^2/\varphi_i,$$

where φ_i^* and φ_i are the experimental and calculated sieving coefficients. The sum is taken over all integer values of the molecular radius such that $0.1 \leq \varphi_i^* \leq 0.9$.

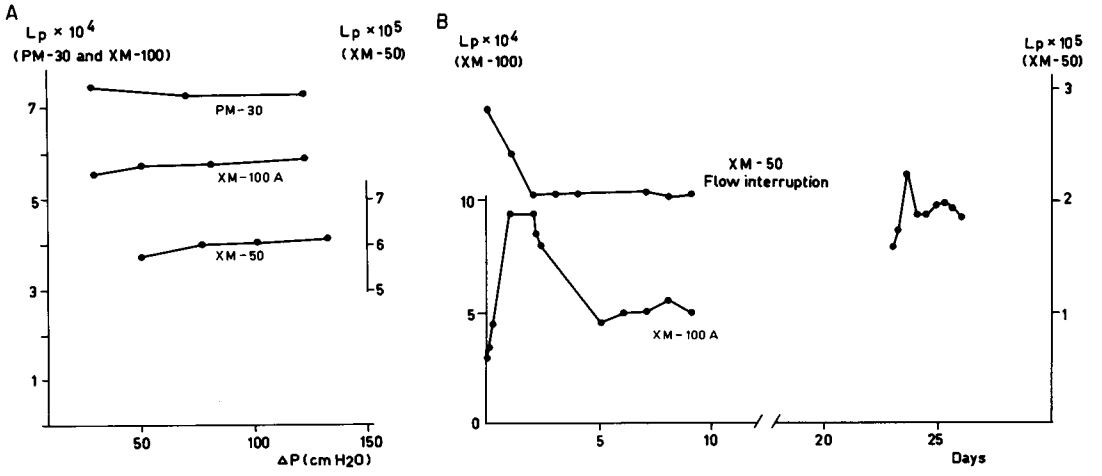

FIGURE 3 (*A*) Conductance of PM-30, XM-50, and XM-100 membrane at different pressures, measured within 6 h of initial pressurization; L_p in ml · min^{-1} · cm^{-1} H_2O · cm^{-2}. (*B*) Time dependence of the conductance of an XM-50 and of an XM-100 membrane.

RESULTS

All calculations were performed with and without the radial correction for K_2/K_1. The results quoted hereunder are those obtained with the radial correction, except for the determination of the filtration pressure from sieving data and Fig. 8, where results obtained with both equations are given.

Conductance

Fig. 3 A shows that the conductance of a new PM-30, XM-50, and XM-100 A membrane, measured with distilled water, is relatively independent of the pressure up to 150 cm H_2O. It usually decreases at higher pressures. However, though the conductance seems to be stable when measured within a span of a few hours, it changes with time (Fig. 3 B, left) to reach a plateau after a few days of continuous flow. During this period, the conductance usually decreases for XM-50 membranes. When the flow is interrupted for several days, then reinstalled (Fig. 3 B, right), a new period of instability occurs. This points to the necessity of allowing a sufficient settling period before stable and reproducible results can be obtained.

For a PM-30 membrane, the mean hydraulic conductance was found to be 60 × 10^{-5} ml/min·cm H_2O·cm^2 membrane. For 6 XM-50, the mean value was 12.5 × 10^{-5} and the range 4.2–27.8. These membranes came from different lots.

For 6 XM-100 membranes, mean value: 66 × 10^{-5}, range: 45–92.

Sieving Curves

Typical sieving curves obtained at different pressures on an XM-50 and an XM-100 membrane are shown in Fig. 4 A and 4 B. As predicted by the theory, the steepest

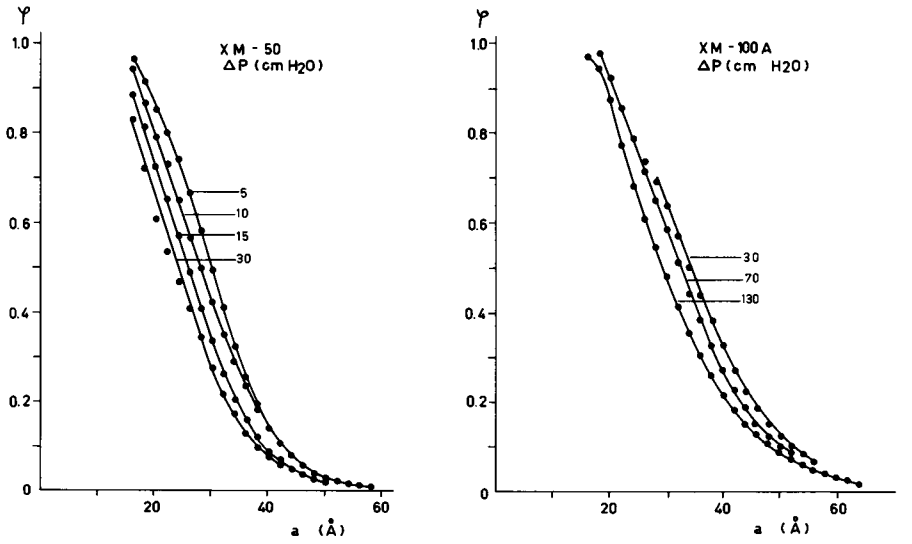

FIGURE 4 Experimental sieving coefficients at different filtration pressures for (*A*) an XM-50 and (*B*) an XM-100 membrane. The lines are drawn by sight.

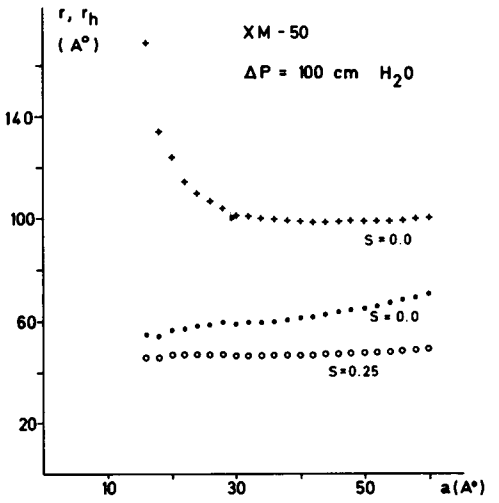

FIGURE 5 Step by step analysis (XM-50); pore radius calculated for each molecular radius. Dots: Isoporous theory; open circles: heteroporous theory; crosses: using Renkin's frictional resistance term for convection.

curves correspond to the lowest pressures and all curves converge for high molecular radii.

Radii of the Pores Calculated by the Isoporous Theory

For an ideal isoporous membrane, φ depends only on ΔP, r, and a. When φ and ΔP are known, it is possible to calculate a value of r for each value of a. The plot of r thus calculated in function of a for a typical experiment is represented in Fig. 5 (dots). As the values of r are relatively constant for a up to 36 Å (for this particular membrane), we can consider that the isoporous theory correctly describes the membrane structure as far as small molecules are concerned. However, for larger molecules, this theory is inadequate and the passage of large molecules is better described by assuming an heteroporous distribution. This will be discussed in the next section.

The use of a weighting factor was necessary in order to give a good overall adjustment between the theoretical and experimental sieving curves. The factor $1/\varphi_i$ was chosen as a compromise giving the best visual fit. $1/\varphi_i^2$ was also tried but gave too much weight to the high molecular size range, where experimental errors are more important than for smaller radii, due to the small concentrations of large molecules in the filtrate.

We have calculated the mean effective pore's radius at different pressures for several membranes. The results are given in Fig. 6 for a typical PM-30, XM-50, and XM-100 membrane. The radius found at different pressures on the same membrane is relatively constant. The experiments of Fig. 6 were performed after several days of continuous flow. When the experiments are done on fresh membranes, just after initial pressurization, less consistent results are obtained for the radius.

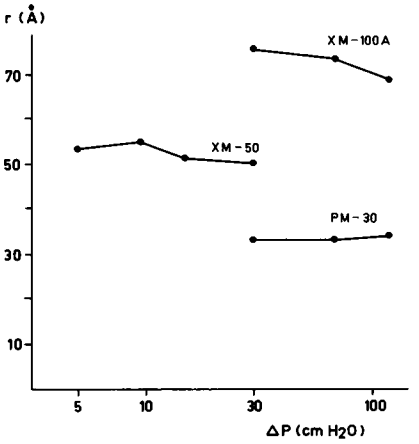

FIGURE 6 Isoporous radii of PM-30, XM-50, and XM-100 membranes at different filtration pressures.

An upper bound on the error of the determinations of the radii was obtained in the following way. The chief cause of error in the experimental results is the variation of the total volume V_t of the chromatography column. Short time fluctuations were observed in addition to a more gradual variation, making it difficult to correct the results completely for this drift though V_t was measured for each chromatography. We estimate that 2 ml is an upper bound on these fluctuations. Consequently, we calculated the sieving coefficients for the experiments of Fig. 6 as if V_t had drifted upward or downward by 2 ml. We then determined the radii under these conditions; these differed by less than 1 Å from the quoted values.

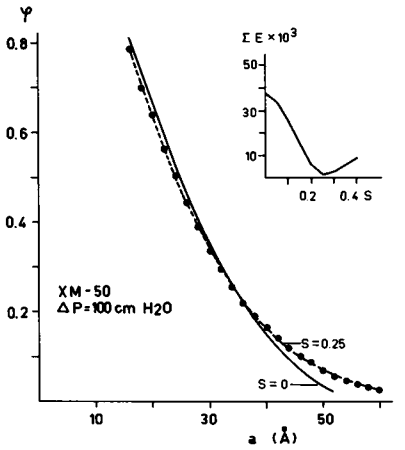

FIGURE 7 (*A*) Theoretical curves with isoporous (solid line) and heteroporous (dashed line) theory, fitted to experimental sieving coefficients (dots). (*B*) $\sum E$ in function of s.

Pore Size Distribution Calculated by the Heteroporous Theory

A better adjustment between theoretical curve and experimental data is obtained when a lognormal pore size distribution function is considered. For example, the values of r_h (median of the distribution) for each value of a in the experiment of Fig. 5 are given by the open circles. The value of s used was obtained by fitting the curve for φ between 0.1 and 0.9. The experimental sieving coefficients (dots) are shown in Fig. 7 A, together with the best theoretical curve with $s = 0$ (isoporous theory) in dashed line and the curve with s optimized (heteroporous theory) in full line. Fig. 7 *B* shows that the sum of errors reaches a minimum value for $s = 0.25$ (r_h is optimized for each value of s).

The median pore radius r_h, the standard deviation of the lognormal distribution s and the mean pore radius r_m (Eq. 10) have been calculated for several membranes and at different pressures. Table I shows the mean values of r_h, s, and r_m for each membrane, together with their SEM. n is the number of sieving curves analyzed for each membrane. As already noted for the conductance, noticeable differences exist between membranes of the same type, but from different lots.

Determination of the Filtration Pressure from Sieving Data

The model described in this paper has been used for several years in our laboratory to determine the effective glomerular filtration pressure in the dog kidney, from the sieving of PVP through the glomerular membrane (1, 5, 22, 24, 25). The glomerular filter was shown to be reasonably isoporous (when molecules of radii between 19 and 37 Å are considered). Thus both the pore radius and the filtration pressure can be calculated by the minimization technique described in the section on computer methods and in ref. 1. This is possible because the effects of r and ΔP on the shape of the curve are different (a variation of r induces a translation of the curve whereas ΔP influences the steepness) (25).

It seemed important to verify the validity of this procedure by experiments on artificial membranes of permeability similar to the glomerular filter (radius approximately 46 Å [5]). The XM-50 seemed the best choice for these experiments and the

TABLE I

MEAN VALUES OF r_h, s, AND r_m FOR DIFFERENT MEMBRANES

Membrane	Lot	n	r_h	s	r_m
			Å	Å	Å
PM-30	165	3	25.9 ± 4.5	0.23 ± .09	28.9 ± 2.9
XM-50	395	7	23.9 ± 0.8	0.45 ± .03	34.4 ± 0.8
XM-50	395	6	28.6 ± 2.2	0.48 ± .02	42.5 ± 1.9
XM-50	186	5	54.3 ± 2.2	0.16 ± .03	57.7 ± 1.3
XM-50	186	5	64.9 ± 2.0	0.04 ± .02	65.3 ± 2.0
XM-50	186	2	63.6 ± 5.8	0.03 ± .02	69.8 ± 5.9
XM-50	186	4	70.1 ± 7.6	0.08 ± .02	71.1 ± 7.0
XM-100 A	93	3	72.4 ± 1.9	0.02 ± .02	72.5 ± 2.1

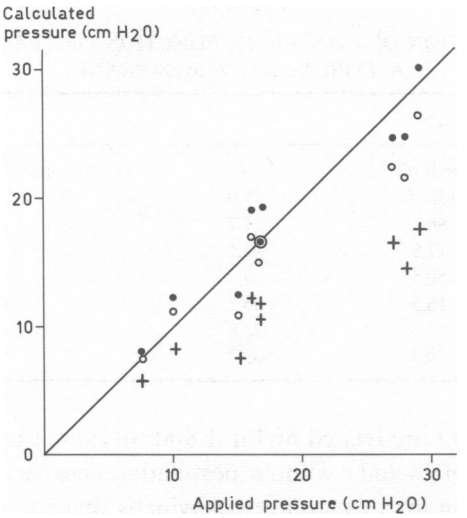

FIGURE 8 Calculated filtration pressures vs. applied pressure for several XM-50 membranes, with the radial variation of K_2/K_1 neglected (dots) or taken into account (open circles). The crosses are the pressures calculated with Renkin's equation. The solid line is the identity line.

sieving curves of PVP at several pressures from 7.5 to 30 cm H_2O (5.5–22 mm Hg) were determined. The values of r_h, s, and ΔP were then calculated. As the effects of ΔP and s on the shape of the sieving curve are similar (Fig. 1 B and 1 C), the accuracy of the determination of ΔP when s is different from zero is poor. Therefore, the results used for the comparison are those obtained on nearly isoporous membranes.

Fig. 8 shows the correlation between the calculated pressures and the applied pressures, measured with the water gauge. The dots are obtained when the radial variation of K_2/K_1 is not taken into account. In this case, the mean value (±SEM) of the ratios of calculated to applied pressure is 1.036 (±0.138). On the other hand, when the radial variation of K_2/K_1 is taken into account the values of the open circles are found. These give the less satisfactory value of 0.927 (±0.132). A comparison between the pairs of ratios shows that the mean of the differences is significantly different from zero (t_s = 9.8; $P < 0.001$).

DISCUSSION

Conductance

The initial variation of the conductance of the membrane is probably due to hydration, but this does not explain the variations after an interruption of flow. The latter are probably caused by mechanical strains due to the pressure on the membrane.

Pore Radii

During the first 24 h after initial pressurization, a change in the (isoporous) radius was often noticed, without corresponding variation in Lp, as in the experiment described in Table II. T is the time since initial pressurization.

TABLE II

VARIATION OF r AND L_p IN FUNCTION OF TIME FOR A TYPICAL XM-50 MEMBRANE

Time	ΔP	r	$L_p \times 10^5$
h	$cm\ H_2O$	$\AA$	$ml \cdot min^{-1} \cdot cm^{-1}\ H_2O \cdot cm^{-2}$
1	135	45.0	11.2
3	88	51.1	11.8
24	27.5	62.5	11.7
27	50.5	59.2	11.3
48	16.5	66.7	10.8
72	7.5	72.8	8.6
96	29.3	67.2	10.9

In our model, Lp and r are related by Eq. 1 and we cannot explain the discrepancy between the variations of Lp and r without postulating unexpected changes in L or N. One possible explanation for this strange behavior is that the radius of the pores is modified only near the surface of the membrane: this would affect the sieving of macromolecules but would leave the bulk water conductivity essentially unchanged. When the conductance is stabilized, the radius of the pores, determined at different pressures, is almost constant (Fig. 6).

The small residual decrease of r with ΔP observed on most membranes is probably due to effects not considered in the model: collisions of molecules with the walls, adsorption, pore tortuosity, etc. It is unlikely that deformation of the macromolecules occurs during transit through the pores. Indeed, at high pressures and flows, the molecules would tend to be stretched by the velocity gradients in the pores. This would facilitate the passage of the larger molecules and increase their φ. This is in contradiction with the experimental results of Figs. 4 A and 4 B which show that the φ are always lower at high pressures.

Concentration polarization would result in the formation, at the upper surface of the membrane, of an unstirred layer with a higher solute concentration than in the

TABLE III

COMPARISON WITH ELECTRON MICROSCOPY

	XM-50		XM-100	
	From EM	From sieving data	From EM	From sieving data
r_h, A °	46	54.3	70	72.4
$w, \AA$	23–64	30–73	30–89	68–76
$\theta \times 10^3$	0.4	3	5.4	16
		(0.6)		(3.2)
$N \times 10^{-8}, cm^{-2}$	5.3	29	29	100
		(5.8)		(20)

EM, electron microscopy; w, width of distribution at half of maximum height. Values of θ and N calculated with L = 1,000 Å; values for L = 200 Å are given in brackets.

bulk. The concentration at the surface of the membrane is determined by the combined effect of (*a*) filtration which brings solute molecules from the bulk to the surface of the membrane; the molecules which are rejected at the entrance of the pores accumulate near the surface; and (*b*) back-diffusion which tends to reduce the concentration gradient between the bulk and the vicinity of the membrane surface. The increase of concentration, compared with the solution, is expected to be more important for large molecules (which are rejected in greater quantities at the entrance of the pores, and which have a smaller diffusion coefficient) and at higher pressures (the number of molecules transported toward the membrane is higher, thus creating a greater gradient). This would again result in higher sieving coefficients for large molecules. It is thus also unlikely that concentration polarization is important in these experiments.

Comparison with Electron Microscopy

The mean values of r_h (50.9 Å for 6 XM-50 membranes and 72.4 Å for the XM-100) are comparable to those found by Preusser (23) with an electron microscope: 46 Å for the XM-50, 70 Å for the XM-100. A more detailed comparison is given in Table III. θ and N are calculated by Eq. 1, using for L 1,000 Å, the minimum value given by Amicon. A better agreement with Preusser's values for θ and N can be obtained by taking for L a much lower value, for example 200 Å. An "effective" length of 200 Å, much smaller than the actual length, can be explained by supposing that the pore is not cylindrical, but is constricted over part of its total length. The results obtained with L = 200 Å are given between brackets.

The discrepancy might also be due to the important differences between the conductances of membranes of different lots; it is thus possible that the membrane studied by Preusser had a conductance, and thus a value of N, much lower than those we tested.

Radial Variation of K_2/K_1

It has not been possible to make a clear choice between the values of $\overline{K_2/K_1}$ calculated by taking into account the radial variation of K_2/K_1 or neglecting this variation because neither of these formulas gives a significantly better adjustment for the whole lot of experiments. The difference between the sieving coefficients calculated with either formula is noticeable only in the middle part of the sieving curve, as shown in Fig. 1 C. Eq. 9, which is theoretically more accurate, was used for the results presented in this article (with the exception of Fig. 8, where both equations are used.

Determination of the Filtration Pressure from Sieving Data

The comparison between the applied pressures and the pressures calculated from the sieving data shows that the method used to calculate the effective glomerular filtration pressure is valid, and that a better estimate is obtained when the radial variation of K_2/K_1 is neglected. The results previously obtained (5) are thus confirmed.

Comparison with Renkin's Equation

We have repeated the calculations of r in function of a using Renkin's frictional resistance term for convection ($1/K_1$ instead of K_2/K_1 in our equation). The re-

sults are shown by the crosses in Fig. 5. The pore radii found are much higher than with our equation; this is due to the greater restriction for convection, as shown in Fig. 1 A. Even with the best value of s (0.0 in this case), the radii of the pores calculated from the sieving coefficients of macromolecules of different sizes are quite different for $a < 35$ Å. We are thus led to the conclusion that Renkin's term does not correctly describe the restriction for small and medium-sized molecules.

The filtration pressures were also calculated with Renkin's equation,by the method described above. The results are given by the crosses in Fig. 8. It is evident that the use of this equation would lead to large errors in the determination of the filtration pressure.

CONCLUSION

The good agreement that can be obtained between the theoretical and experimental sieving coefficients, particularly with the heteroporous model, lends strong support to the transport equation established to describe the sieving of macromolecules through both artificial and biological membranes.

This equation may therefore be used to determine the transcapillary filtration pressure. However, taking into account the radial variation of K_2/K_1 does not seem necessary as it does not increase the accuracy of the results.

We wish to express our gratitude to Professor P. P. Lambert who initiated this study and supported it throughout. We thank Professor A. Verniory for his advice in the statistical calculations. We are indebted to Dr. P. Decoodt for providing us with the Tauros minimization subroutine used in all our calculations. It was extracted from the MINUITS program of the CERN Computer 6000 Series Program Library; Long Write Up D 506.

The help of Mme. M. Lammens-Verslype for the chromatographic analyses is gratefully acknowledged.

Support for this study was provided by the Fonds de la Recherche Scientifique Médicale of Belgium (grant 1197).

Received for publication 20 November 1975 and in revised form 20 July 1976.

REFERENCES

1. VERNIORY, A., R. DU BOIS, P. DECOODT, J. P. GASSEE, and P. P. LAMBERT. 1973. Measurement of the permeability of biological membranes. Application to the glomerular wall. *J. Gen. Physiol.* **62**:489.
2. PAPPENHEIMER, J. R., E. M. RENKIN, and L. M. BORRERO. 1951. Filtration, diffusion and molecular sieving through peripheral capillary membranes. *Am. J. Physiol.* **167**:13.
3. BEAN, C. P. 1972. The physics of porous membranes. I. *In* Membranes—A Series of Advances. Vol. 1. G. Eisenman, editor. Marcel Dekker, Inc., New York.
4. CHANG, R. L. S., C. R. ROBERTSON, W. M. DEEN, and B. M. BRENNER. 1975. Permselectivity of the glomerular capillary wall to macromolecules. I. Theoretical considerations. *Biophys. J.* **15**:861.
5. LAMBERT, P. P., R. DU BOIS, P. DECOODT, J. P. GASSEE, and A. VERNIORY. 1975. Determination of glomerular intracapillary and transcapillary pressure gradients from sieving data. II. A physiologic study in the normal dog. *Pflügers Arch. Eur. J. Physiol.* **359**:1.
6. BECK, R. E., and J. S. SCHULTZ. 1972. Hindrance of solute diffusion within membranes as measured with microporous membranes of known pore geometry. *Biochim. Biophys. Acta.* **255**:273.
7. RENKIN, E. M. 1954. Filtration, diffusion and molecular sieving through porous cellulose membranes. *J. Gen. Physiol.* **38**:225.

8. GOLDSMITH, H. L., and S. G. MASON. 1962. The flow of suspensions through tubes. I. Single spheres, rods and discs. *J. Colloid Sci.* **17**:448.
9. ANDERSON, J. L., and J. A. QUINN. 1974. Restricted transport in small pores. A model for steric exclusion and hindered particle motion. *Biophys. J.* **14**:130.
10. HABERMAN, W. L., and R. M. SAYRE. 1958. Motion of rigid and fluid spheres in stationary and moving liquids inside cylindrical tubes. David Taylor Model Basin Report no. 1143. Department of the Navy, Washington, D.C.
11. WANG, H., and R. SKALAK. 1969. Viscous flow in a cylindrical tube containing a line of spherical particles. *J. Fluid Mech.* **38**:75.
12. PAINE, L. P., and P. SCHERR. 1975. Drag coefficients for the movement of rigid spheres through liquid-filled cylindrical pores. *Biophys. J.* **15**:1087.
13. FAMULARO, J. 1962. D.Eng.Sci. Thesis. New York University, New York.
14. HAPPEL, J. and H. BRENNER. 1965. Low Reynolds Number Hydrodynamics. Prentice-Hall, Inc., Englewood Cliffs, N.J.
15. BRENNER, H., and J. HAPPEL. 1958. Slow viscous flow past a sphere in a cylindrical tube. *J. Fluid Mech.* **14**:195.
16. BRENNER, H., and P. M. BUNGAY. 1971. Rigid-particle and liquid-droplet models of red cell motion in capillary tubes. *Fed. Proc.* **30**:1565.
17. GREENSTEIN, T., and J. HAPPEL. 1968. Theoretical study of the slow motion of a sphere and a fluid in a cylindrical tube. *J. Fluid Mech.* **34**:705.
18. BUNGAY, P. M., and H. BRENNER. 1973. Pressure drop due to the motion of a sphere in proximity to the wall bounding a Poiseuille flow. *J. Fluid Mech.* **60**:81.
19. BUNGAY, P. M. and H. BRENNER. 1973. The motion of a closely-fitting sphere in a fluid-filled tube. *Int. J. Multiphase Flow.* **1**:25.
20. LEVITT, D. G. 1975. General continuum analysis of transport through pores. I. Proof of Onsager's reciprocity postulate for uniform pore. *Biophys. J.* **15**:533.
21. GOLDMAN, A. J., R. G. COX, and H. BRENNER. 1967. Slow viscous motion of a sphere parallel to a plane wall. I. Motion through a quiescent fluid. *Chem. Eng. Sci.* **22**:637.
22. LAMBERT, P. P., A. VERNIORY, J. P. GASSEE, and P. FICHEROULLE. 1972. Sieving equations and effective glomerular filtration pressure. *Kidney Int.* **2**:131.
23. PREUSSER, H. J. 1972. The ultrastructure of some fine-pored types of membrane filters. (German.) *Kolloid Z.Z. Polym.* **230**:133.
24. GASSEE, J. P., P. DECOODT, A. VERNIORY, and P. P. LAMBERT. 1974. Autoregulation of effective glomerular filtration pressure. *Am. J. Physiol.* **226**:616.
25. DU BOIS, R., P. DECOODT, J. P. GASSEE, A. VERNIORY, and P. P. LAMBERT. 1975. Determination of glomerular intracapillary and transcapillary pressure gradients from sieving data. I. A mathematical model. *Pflügers Arch. Eur. J. Physiol.* **356**:299.